ICARUS 109, 352–366 (1994)

Laboratory Measurements of the Microwave Properties of H_2S under Simulated Jovian Conditions with an Application to Neptune

DAVID R. DEBOER AND PAUL G. STEFFES

School of Electrical and Computer Engineering, Georgia Institute of Technology, Atlanta, Georgia 30332-0250
E-mail: gt7952a@prism.gatech.edu

Received November 22, 1993; revised April 29, 1994

H_2S opacity may significantly affect the brightness temperatures of Uranus and Neptune due to possible depletion of ammonia in the tropospheres of those planets (de Pater *et al.* 1991, *Icarus* 91, 220–233). Though the rotational line centers of H_2S are in the millimeter wavelength region, significant absorption is also present at centimeter wavelengths due to pressure broadening of the lines. Accordingly, the properties of H_2S under Jovian conditions have been measured in order to constrain further the constituents' abundances on these planets. These absorptivity measurements show values that are significantly greater than values predicted by the Van Vleck–Weisskopf models traditionally used at centimeter wavelengths. In order to better model the opacity due to H_2S under Jovian conditions a Ben-Reuven lineshape formalism has therefore been developed and is presented. This formalism provides a possible constraint on the relative abundances of H_2S and NH_3 on Neptune based on Voyager 2 radio occultation results (Lindal 1992, *Astron. J.* 103, 967–982). © 1994 Academic Press, Inc.

1. INTRODUCTION

The Jovian planets are a window to understanding the primordial cloud from which our solar system was born in that they retain a large portion of their original composition due to their large bulk. In addition, a significant fraction of their mass lies in the observable atmosphere, making these planets a good laboratory for study. Investigating these planets therefore can give a better understanding of the formative processes of planets. Such investigation is facilitated by laboratory measurements and computer modeling.

Laboratory measurements are vital in order to properly interpret observational data, such as results from radio occultation experiments and radio astronomical observations, as they give the behavior of critical molecules under conditions similar to those on the gas giants. An ongoing program to make these measurements has been conducted at the Georgia Institute of Technology. This paper presents the results for measurements of hydrogen sulfide (H_2S) in a hydrogen-helium atmosphere at relatively high pressures and low temperatures. A computer model for these gas giants has also been developed and some preliminary results are presented which tend to support the assertion that H_2S may be the dominant microwave absorber in the upper troposphere of Neptune.

2. LABORATORY CONFIGURATION AND PROCEDURES

The laboratory configuration used in this work is identical to that used in Steffes and Jenkins (1987) with a few small refinements. The objective of this laboratory setup is to simulate Jovian conditions and measure the microwave properties of gases. It consists of two subsystems: (1) the outer planet atmosphere simulator and (2) the microwave measurement subsystem.

The outer planet atmosphere simulator consists of a hermetically sealed stainless steel pressure vessel which in turn is placed inside a temperature chamber capable of reaching temperatures as low as 150 K. The pressure vessel is connected to three gas cylinders via stainless steel tubing with sufficient stop valves so that every piece of the network may be isolated to aid in the detection of leaks, as well as for safety considerations. A combustible gas detector and a water bubble technique were used to detect and locate leaks within the system. When properly sealed, the system can safely contain pressures exceeding 7 bars and can sustain this pressure with no discernible leaks over a period of hours. A roughing vacuum pump was also connected to the vessel to evacuate the chamber and is capable of producing a vacuum of 3 Torr. For pressure measurements between 1 and 800 Torr, a digital thermocouple vacuum gauge was used, while for higher pressures an analog gauge was used with an accuracy of 0.2 atm throughout its usable range.

The microwave subsystem consists of two cylindrical silver-plated cavity resonators which both reside within the pressure vessel. The larger of the two resonators was

0019-1035/94 $6.00

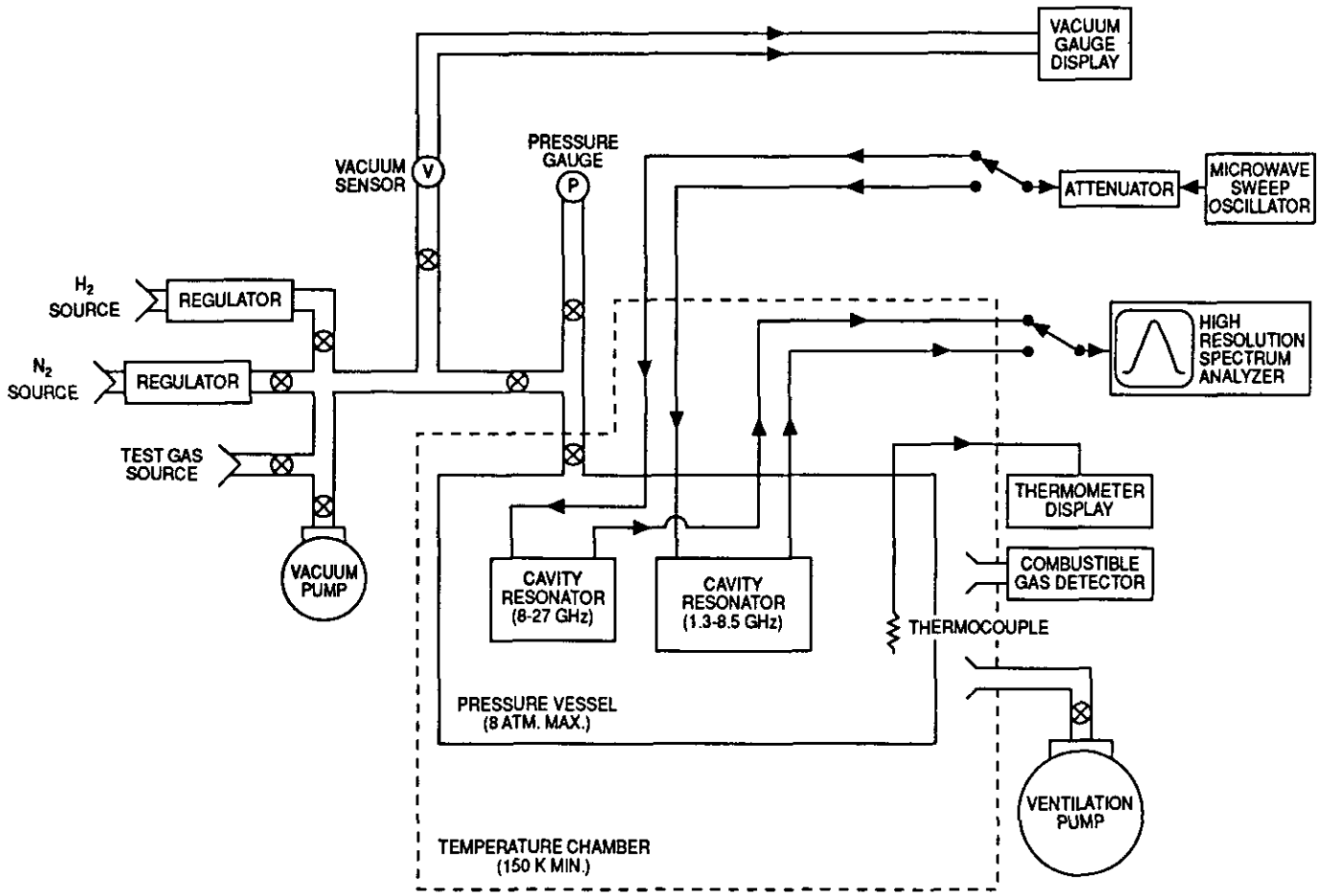

FIG. 1. Block diagram of the outer planet simulator and microwave subsystem.

used for the S band data (2.25 GHz or 13.3 cm) and the X band (8.5 GHz or 3.5 cm) measurements, which correspond to TE_{013} and TE_{067} modes respectively. The small resonator was used for the K band (21.7 GHz or 1.38 cm) measurement, which corresponds to the TE_{034} mode. Mode suppression slots are incorporated in each resonator to block the degenerate TM modes, which have lower quality factors. Two HP 8690 microwave sweep oscillators are used to generate the input signal in the three bands and a high resolution HP 8562B spectrum analyzer is used to measure the output signal. Figure 1 shows a block diagram of the simulator and microwave subsystem.

3. DATA REDUCTION AND EXPERIMENTAL UNCERTAINTY

To calculate the power absorption from the quality factor of a gas, Q_g, recall that

$$\frac{\alpha}{\beta} = 2\sqrt{\frac{\sqrt{1+(\varepsilon''/\varepsilon')^2}-1}{\sqrt{1+(\varepsilon''/\varepsilon')^2}+1}} \tag{1}$$

(see, e.g., Reitz *et al.* 1980), where $\beta = 2\pi/\lambda$, λ is the wavelength with the gas present, α is the absorption in optical depths per unit length, and $\varepsilon = \varepsilon' - j\varepsilon''$ is the complex permittivity. (Note that 1 optical depth/unit length = 0.5 Nepers/unit length = 4.343 dB/unit length.) Since $\varepsilon'' \ll \varepsilon'$ for gases in the microwave region, this reduces to

$$\frac{\alpha}{\beta} \approx \frac{\varepsilon''}{\varepsilon'}. \tag{2}$$

Note that the quality factor due to a lossy gas is given by $Q_g = \varepsilon'/\varepsilon''$ (see, for example, Pozar 1990) and therefore

$$\alpha \approx \frac{\beta}{Q_g} = \frac{2\pi}{\lambda}\frac{1}{Q_g}. \tag{3}$$

To determine Q_g we must examine the total quality factor of the resonator and how it changes in the presence of a lossy gas. The total (or measured) quality factor of a gas-filled (or loaded) resonator can be given by

$$\frac{1}{Q_T} = \frac{1}{Q_C} + \frac{1}{Q_g} + \frac{1}{Q_{E(1)}} + \frac{1}{Q_{E(2)}} \tag{4}$$

(Matthaei *et al.* 1980), where Q_T is the total quality factor, Q_C is the quality factor of just the cavity, and Q_E is the external quality factor (that is, the Q characterizing the coupling to and from the cavity). For Q_E, the 1,2 subscripts denote the input and output ports of the resonator. Since a symmetrical cavity is used, assume that $Q_{E(1)} = Q_{E(2)} \equiv Q_E$. Additionally, Ginzton (1957) shows that

$$\frac{\sqrt{t}}{2Q_T} = \frac{1}{Q_E}, \tag{5}$$

where t is the transmissivity of the resonator at resonance. Note that t assumes a lossless gas, but it was found that for relatively low loss gases (such as H_2S), the difference is negligible for most resonators. Note: The value of t for most resonators is on the order of 10^{-3} or less.

If there is no gas in the resonator (referred to as an unloaded resonator), or if the gas is lossless, then $1/Q_g = 0$, and substituting Eq. (5) into the total quality factors for a loaded and unloaded resonator and then subtracting yields

$$\frac{1}{Q_g} = \frac{1 - \sqrt{t_l}}{Q_{Tl}} - \frac{1 - \sqrt{t_u}}{Q_{Tu}} + \frac{1}{Q_{Cu}} - \frac{1}{Q_{Cl}}, \tag{6}$$

where the subscripts l and u refer to loaded and unloaded resonators respectively.

Note that Q_C takes losses of the resonator itself into account (not counting the loss from the opacity of the gas), and is, unfortunately not a directly measurable component. Imperfectly conducting walls and leakage from the resonator (through mode suppression slits for example) are examples of contributors to the Q_C term. For imperfectly conducting walls, the ratio of the loaded and unloaded Q_C's for a cylindrical resonator goes as the square root of the ratio of the different center frequencies, which is very nearly unity if the difference in refractivity is not exceedingly large. Likewise, for leakage, the ratio of the Q_C's would go approximately as the ratio of the different center wavelengths and, for moderate refractivity differences, would again be nearly unity. In this case, therefore, to a good approximation $Q_{Cu} \approx Q_{Cl}$. The expression for the quality factor of the gas is then

$$\frac{1}{Q_g} = \frac{1 - \sqrt{t_l}}{Q_{Tl}} - \frac{1 - \sqrt{t_u}}{Q_{Tu}} \tag{7}$$

and therefore

$$\alpha = 4.343 \frac{2\pi}{\lambda} \left(\frac{1 - \sqrt{t_l}}{Q_{Tl}} - \frac{1 - \sqrt{t_u}}{Q_{Tu}} \right) \text{ dB/m} \tag{8}$$

with λ in meters.

For a considerable difference in refractivity between the vacuum and gas, the assumption that $Q_{Cl} = Q_{Cu}$, however, begins to break down. This is referred to as dielectric loading of the resonator (see, e.g., Joiner *et al.* 1989 or Spilker 1993) and is due to the increase of disparity between the loaded and unloaded cavity quality factors (Q_C) leading to errant absorptivity results. One solution is to recall that $1/Q_g = 0$ for a lossless gas as well as for a vacuum and thus the same expression (Eq. (8)) can be used if a lossless gas is used for the unloaded terms Q_{Tu} and t_u. If the lossless gas is used in lieu of a vacuum for the unloaded resonator, and the refractivity can be matched to the lossy gas, then the effects of dielectric loading will be negated. Furthermore, if the lossless gas is used for the unloaded terms then $t_l \approx t_u$ and the numerators can be factored as a single scaling term.

To match the refractivity, the resonant center frequency is measured at vacuum then with the test gas. A vacuum is again drawn and a lossless calibration gas is added so that the shift in the center frequency is identical to the test gas relative to the center frequency at vacuum. This method to remove the effects of dielectric loading was done using first a H_2–He mixture in the early experiments, but then N_2 was used when it was found that the relatively large refractivity from H_2S could not be matched using only hydrogen and helium. Even with nitrogen, the refractivity could not always be perfectly matched at the higher pressures.

The above analysis assumes the ability to perfectly measure the quality factor of a resonator. This is, of course, not possible. To understand the error incurred it is instructive to examine how the quality factor is measured. Recall that the quality factor is 2π times the ratio of the time-averaged energy stored to the energy lost per cycle within the resonator system. This can be expressed as $Q = f_0/\Delta f$, where f_0 is the center frequency of the resonance line and Δf is the measured bandwidth. The center frequency can be determined very accurately and typically changes little over many measurements (less than 0.01%). The greater source of error in estimating the Q of a resonator comes from the bandwidth measurements. The half power bandwidth is determined essentially by eye-fitting a curve over a noisy resonant line and measuring with a spectrum analyzer. Additional data taken in March of 1994 utilizes a computer interface which reads, smooths and fits the 3 dB and center points. Assuming uncorrelated measurement error (an unbiased observer) the best estimation of the bandwidth is obviously the mean of many measurements. Therefore,

TABLE I
Instrument Uncertainty for the Frequency Bands

	σ_0 [kHz]	σ_Δ [Hz]
S band	25	240
X band	90	800
K band	320	4815

$$\Delta f \approx \frac{1}{N}\sum_{i=1}^{N}\Delta f_i \tag{9}$$

where Δf_i are the individual bandwidth measurements. To determine the accuracy of the measurements we calculate the sample variance,

$$S_N^2 = \frac{1}{N-1}\sum_{i=1}^{N}(\Delta f_i - \Delta f)^2, \tag{10}$$

and finally the variance of our estimate from the "true" bandwidth due to electrical noise,

$$\sigma_N^2 = B\frac{S_N^2}{N}, \tag{11}$$

where $B = 1.88$ gives us the 90% confidence level for the 10 measurements taken per data point for the data prior to 1994, and $B = 1.77$ gives the same confidence level for the 20 measurements taken in March 1994 (Papoulis 1991).

This gives an estimate of the random electrical noise associated with the measurement, but there are also instrument errors which must be taken into consideration as well. These stem from the limited accuracy of the spectrum analyzer and may be calculated as follows (Hewlett–Packard Corporation, 1986):

$$\sigma_0 \approx 10^{-5}f_0 + 0.15\text{RBW} + 0.05\text{SPAN} + L_0 + 250 \quad \text{Hz} \tag{12}$$

$$\sigma_\Delta \approx 10^{-5}\Delta f + 200N_H + 4L_{BW} \quad \text{Hz}. \tag{13}$$

Here σ_0 is the standard deviation of the center frequency measurement due to the spectrum analyzer accuracy, σ_Δ the standard deviation of the bandwidth measurement, SPAN is the frequency coverage of the spectrum analyzer display, RBW is the resolution bandwidth of the spectrum analyzer, L_0 and L_{BW} are the least significant digits of the two measurements, and N_H is the harmonic number. All quantities are given in hertz except N_H, which is the integer number of the harmonic used for mixing the signal down to baseband. How these factors contribute to the uncertainty in the measured absorptivity is discussed in depth in the Appendix. Table I gives the values for these instrument uncertainty terms.

Another quantity that results from these measurements is the microwave refractivity of the gas mixture, which is defined as the refractive index less one multiplied by 10^6,

$$N_R = 10^6(n-1). \tag{14}$$

The refractive index, n, is the ratio of the measured center frequency in a vacuum and the center frequency with the gas present, so the refractivity can be written (Tyler and Howard 1969)

$$N_R = 10^6\frac{f_v - f_g}{f_g}. \tag{15}$$

To separate the contributions from the various gases, note that the refractivity is additive for a mixture of ideal gases. Refractivity measurements therefore were taken for the H_2–He mixture and also the H_2S–H_2–He mixture to isolate the refractivity due solely to H_2S. This yields a density normalized value for the H_2S refractivity of 8.85×10^{-17} N-units/molecules/cm^3, which is independent of frequency over the range of measurement.

4. RESULTS

4.1. Experimental

Data were taken on eight separate occasions at three different temperatures and three different pressures at three different frequencies prior to 1994 and again three more times in March of 1994 at various pressures, two temperatures, and the same three frequencies. A custom premixed, constituent analyzed mixture from Matheson Gas Company was used with an uncertainty of 2% of the stated mixing ratio, though the measurements at 193 K

TABLE II
Summary of H_2S Mixtures Used in Each Experiment

		Mixture (%)		
Date	Temperature	H_2	He	H_2S
May 5, 1993	193 K	93.03	3.02	3.95
June 2, 1993	193 K	93.14	2.94	3.92
April 21, 1993	213 K	79.09	9.07	11.84
June 9, 1993	213 K	79.03	8.98	11.99
February 26, 1992	297 K	79.00	9.00	12.00
January 29, 1993	291 K	79.00	8.99	12.01
February 5, 1993	293 K	79.00	8.99	12.01
June 21, 1993	293 K	79.03	8.98	11.99
March 23, 1994	212 K	79.03	8.98	11.99
March 25, 1994	298 K	79.03	8.98	11.99
March 28, 1994	212 K	79.03	8.98	11.99

required dilution with H_2 gas to prevent condensation. This contributed a corresponding increase in uncertainty of the mixing ratio, resulting in 14% uncertainty in the stated mixing ratio.

Table II summarizes the mixtures used in each experiment. Table III summarizes the results for the measured absorption and compares them to the formalism developed below. Note that the quoted error for the measured value (column 5 in Table III) is σ from the appendix (Eq. (30)) and the formalism error (column 7) is the number of σ's off the measured value. Figures 2–5 represent the results graphically for the three temperatures. Note that the data at S band taken prior to 1994 have not been included in the figures due to the interference of a spurious mode which yielded artificially large absorptivities. This problem was corrected for the March 1994 measurements, and more consistent results were obtained. Furthermore, many of the data at 2 bars are not included since the absorptivity at low pressures tends to lie well below the sensitivity of the system.

Looking at the data it is obvious that some problems exist. The error bars are comparatively large for some of the data, especially at room temperature. This is due to the fact that the low opacity values of H_2S under these conditions lie near the sensitivity level of the system (which are indicated in Figs. 2–5). More troubling are the instances when the opacity at one pressure is greater than the opacity under similar conditions at some greater pressure, which is clearly unphysical under these conditions. Again, this is likely due to the measured quantities being near the level of sensitivity. Note that for instances of the greatest opacity (the data at the higher pressures at 213 K) the error bars are small and the data generally consistent.

4.2. *Formalism for H_2S Microwave Opacity*

To determine an analytical formalism to predict H_2S opacity, note that as a function of frequency the absorption for a collisionally broadened gas can be written

$$\alpha = \sum_j A_j \pi \Delta\nu_j F_j(\nu, \nu_{0j}, \ldots) \quad \text{cm}^{-1}, \tag{16}$$

where A_j is the absorption at the line center, $\Delta\nu_j$ is the linewidth, and $F_j(\nu, \nu_{0j}, \ldots)$ is the lineshape function for line j. See, for example, Townes and Schawlow (1955).

For H_2S, A_j is calculated from the Poynter/Pickett catalog (Poynter and Pickett 1985) and lines up to 1200 GHz are included. A_j can be expressed as

$$A_j = \frac{nS_j(T)}{\pi\Delta\nu_j} \quad \text{cm}^{-1}, \tag{17}$$

where $n = P/k_BT$ molecules/cm^3 is the number density, $S_j(T)$ is the intensity, and $k_B = 1.38 \times 10^{-16}$ erg/K is Boltzmann's constant. The intensity is derived from a measured intensity at a reference temperature T_0 as

$$\begin{aligned} S(T) &= S(T_0)\left(\frac{T_0}{T}\right)^{\eta} \frac{e^{-hcE_l/kT} - e^{-hcE_h/kT}}{e^{-hcE_l/kT_0} - e^{-hcE_h/kT_0}} \\ &\approx S(T_0)\left(\frac{T_0}{T}\right)^{\eta+1} e^{-(hc/k)E_l(1/T-1/T_0)}, \end{aligned} \tag{18}$$

where E_h and E_l are the upper and lower state energies in cm^{-1}, respectively. The η temperature dependence stems from the partition function, where $\eta \approx \frac{3}{2}$ for nonlinear and symmetric-top molecules and 1 for linear molecules. Putting this all together yields

$$A_j = \frac{10^6 P(\text{bar})}{\pi k_B T \Delta\nu_j(\text{cm}^{-1})}\left(\frac{T_0}{T}\right)^{\eta+1} S_j(T_0) e^{-(hc/k)E_{lj}(1/T-1/T_0)} \quad \text{cm}^{-1}. \tag{19}$$

This expression requires $S_j(T_0)$ to be in units of cm^{-1}/molecule/cm^2, whereas Poynter and Pickett quote $S(T_0)$ in units of nm^{2}MHz, which can be converted to the appropriate units by dividing by the factor 2.9979×10^{18}.

The linewidth for a gas mixture can be calculated as

$$\Delta\nu_j = \sum_i \Delta\nu_{ij}^0 P_i \left(\frac{T_0}{T}\right)^{\xi_{ij}} \quad \text{GHz}, \tag{20}$$

where $\Delta\nu_{ij}^0$ is the line broadening parameter for gas i and line j in GHz/bar, P_i is the partial pressure of gas i in bars, and ξ_{ij} is the line broadening parameter temperature dependence for gas i and line j. $\Delta\nu_{ij}^0$ and ξ_{ij} are parameters of the spectral lines and must be determined experimentally.

To get bounds on the temperature dependence of the linewidth, ξ, follow Townes and Schawlow (1955) and note that

$$\Delta\nu \propto n\upsilon\sigma \propto \frac{1}{T}\sqrt{T}\sigma, \tag{21}$$

where n is the number density, $\upsilon = \sqrt{2kT/m}$ is the velocity, and σ is the collision cross-section. The collision cross-section, σ, is related to the force law between molecules, which is of the form $1/r^m$, and the velocity. Substituting these in (21) yields

$$\Delta\nu \propto T^{-(m+1)/2(m-1)} = T^{-\xi}, \tag{22}$$

where $1 < m < \infty$. In the "billiard ball" case (assuming hard sphere collisions), $m = \infty$ and $\Delta\nu \propto 1/\sqrt{T}$, while for

TABLE III
Centimeter Wavelength Laboratory Measurements of H_2S

Date	T [K]	P [bars]	ν [GHz]	α measured [dB/km]	α calc [dB/km]	error [σ]
5/5/93	193	6.17	2.25	0.025 ± 0.057	0.052	-0.47
			8.5	0.951 ± 0.200	0.749	1.01
		4.17	2.25	≤ 0.026	0.024	—
			8.5	0.221 ± 0.192	0.343	-0.63
			21.7	4.812 ± 1.319	2.259	1.94
		2.03	8.5	0.413 ± 0.193	0.081	1.72
			21.7	2.867 ± 1.230	0.537	1.89
6/2/93	193	6.21	2.25	≤ 0.045	0.052	—
			8.5	0.675 ± 0.220	0.754	-0.36
		4.10	2.25	≤ 0.057	0.023	—
			8.5	0.398 ± 0.192	0.329	0.36
			21.7	2.518 ± 1.163	2.167	0.32
		2.03	2.25	0.050 ± 0.058	0.006	0.76
			21.7	2.019 ± 1.234	0.532	1.20
4/21/93	213	6.17	2.25	0.201 ± 0.058	0.121	1.38
			8.5	1.876 ± 0.202	1.739	0.68
		4.17	2.25	0.108 ± 0.057	0.056	0.91
			8.5	0.755 ± 0.196	0.798	-0.22
		2.03	2.25	0.106 ± 0.057	0.013	1.62
			8.5	0.504 ± 0.219	0.190	1.43
			21.7	1.669 ± 1.404	1.250	0.30
6/9/93	213	6.21	2.25	0.215 ± 0.056	0.125	1.61
			8.5	1.828 ± 0.213	1.788	0.18
			21.7	11.705 ± 1.294	11.763	-0.05
		4.10	2.25	0.090 ± 0.057	0.054	0.63
			8.5	0.947 ± 0.199	0.783	0.82
			21.7	5.731 ± 1.536	5.149	0.38
		2.03	8.5	0.360 ± 0.191	0.193	0.88
			21.7	2.026 ± 1.067	1.270	0.71
2/26/92	297	6.17	2.25	0.154 ± 0.060	0.036	1.98
			8.5	0.871 ± 0.181	0.556	1.72
			21.7	1.263 ± 1.165	3.551	-1.96
1/29/93	291	6.17	2.25	0.154 ± 0.082	0.039	1.40
			8.5	0.149 ± 0.230	0.560	-1.78
		4.10	2.25	0.062 ± 0.070	0.017	0.64
			8.5	0.161 ± 0.212	0.250	-0.42
		2.03	2.25	≤ 0.060	0.004	—
			8.5	≤ 0.173	0.061	—
2/5/93	293	6.10	8.5	0.626 ± 0.217	0.535	0.42
		4.10	8.5	0.418 ± 0.194	0.243	0.90
6/21/93	293	6.17	2.25	0.118 ± 0.060	0.038	1.34
			8.5	0.513 ± 0.238	0.546	-0.14
			21.7	1.458 ± 1.431	3.587	-1.48
		4.10	2.25	0.015 ± 0.060	0.017	-0.03
			8.5	0.299 ± 0.199	0.242	0.30
			21.7	2.927 ± 1.328	1.590	1.00
3/23/94	212	5.84	2.25	0.107 ± 0.044	0.112	-0.114
			8.5	1.581 ± 0.145	1.760	-1.234
			21.7	10.721 ± 0.694	10.606	0.166
		5.22	2.25	0.035 ± 0.044	0.090	-1.250
			8.5	1.206 ± 0.144	1.290	-0.583
			21.7	10.700 ± 0.692	8.486	3.199
		4.12	2.25	0.106 ± 0.044	0.056	1.136
			8.5	0.700 ± 0.144	0.804	-0.722
			21.7	7.661 ± 0.686	5.294	3.450
		2.05	8.5	0.036 ± 0.145	0.200	-1.131
			21.7	3.138 ± 0.641	1.319	2.838
3/25/94	298	5.77	2.25	0.038 ± 0.044	0.031	0.159
			8.5	0.372 ± 0.140	0.449	-0.550
			21.7	2.005 ± 0.721	2.951	-1.312
		4.12	2.25	0.055 ± 0.044	0.016	0.886
			8.5	0.223 ± 0.140	0.229	-0.043
			21.7	1.586 ± 0.710	1.506	0.113
3/28/94	212	4.46	2.25	0.068 ± 0.044	0.066	0.045
			8.5	0.859 ± 0.146	0.942	-0.567
			21.7	4.712 ± 0.624	6.199	-2.383

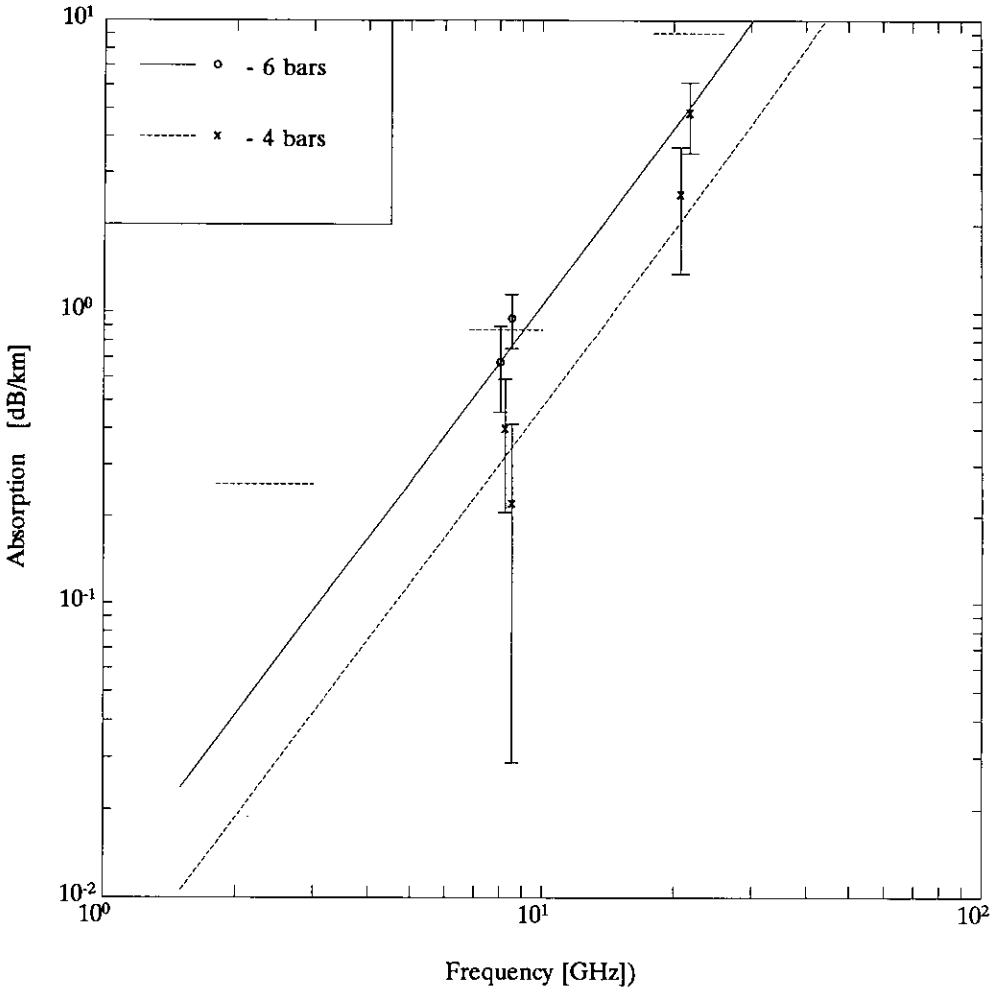

FIG. 2. H_2S attenuation under outer planet atmospheric conditions at 193 K. The theoretical curves are calculated from the Ben-Reuven lineshape function derived in this paper. The data points have been spread about the actual frequency for clarity. The S band data are not included due to the presence of a spurious mode causing artificially elevated opacity readings. The 2-bar data are not included since they lie well below the sensitivity level of the system. The horizontal dashed lines show the estimated average system sensitivity levels at the three bands.

ammonia ($m = 3$) $\Delta\nu \propto 1/T$. Note that $m = 3$ (a dipole) is a lower limit for a neutral gas and hence $0.5 < \xi < 1.0$.

Ben-Reuven (1966) derives a general lineshape for pressure broadening suitable for a range of conditions. In addition to assuming only binary collisions of negligible duration, he also includes terms appropriate for cases where the line width of an individual line is an appreciable fraction of the line center frequency. This shape is expressed by

$$F(\nu, \nu_0, \gamma, \zeta, \delta) = \frac{2}{\pi}\left(\frac{\nu}{\nu_0}\right)^2 \frac{(\gamma - \zeta)\nu^2 + (\gamma + \zeta)[(\nu_0 + \delta)^2 + \gamma^2 - \zeta^2]}{[\nu^2 - (\nu_0 + \delta)^2 - \gamma^2 + \zeta^2]^2 + 4\nu^2\gamma^2} \quad 1/\text{cm}^{-1}, \tag{23}$$

where $\gamma = \Delta\nu$ is the linewidth, ζ the coupling element, and δ the pressure shift term.

The parameters at our disposal for fitting the laboratory measurements are seen to be $\Delta\nu_{ij}^0$, ζ, ξ, and δ and are determined empirically. A simplex fitting code similar to that used by Spilker (1990) was written with the aid of Press *et al.* (1992) to analyze the data and produce a formalism. This was used to generate the first estimates of the unresolved parameters. Full use of this code in determining an optimal formalism based on the laboratory measurements however was hampered by two major problems: (1) the spread in and the nature of the data (e.g., the unphysical results and the comparatively large error bars under some conditions) and (2) not enough individual parameters being varied (we did not, for example, vary the constituent make-up of our test gas except for the measurements at 193 K). Attempts to develop a weighting scheme for the data for use in the computer code quickly grew unwieldy and artificial. The method finally used to determine the unresolved parameters was

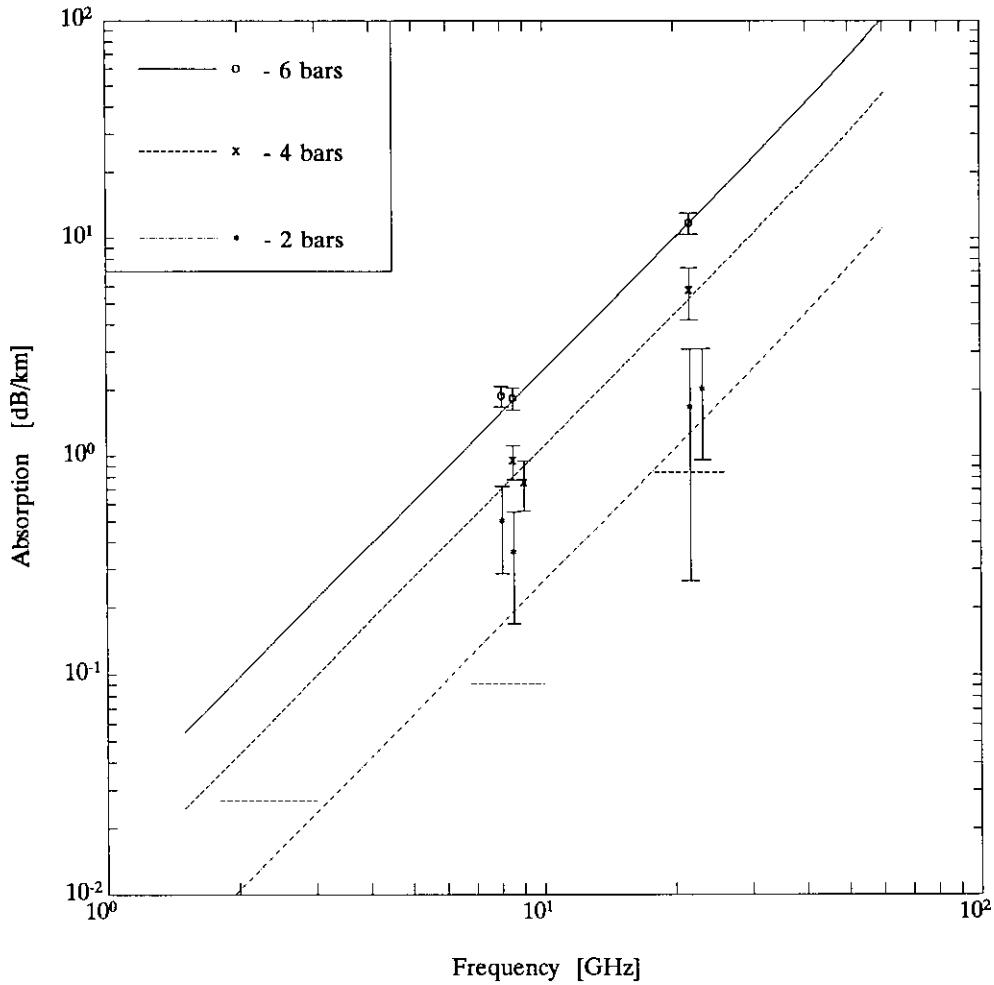

FIG. 3. H_2S attenuation under outer planet atmospheric conditions at 213 K. The theoretical curves are calculated from the Ben-Reuven lineshape function derived in this paper. The data points are data taken prior to 1994 and have been spread about the actual frequency for clarity. The horizontal dashed lines show the estimated average system sensitivity levels at the three frequency bands.

to try many, many variations, plot them, and determine the best fit by eye. Of course, many of the parameters can be constrained by the previous work of others. The obtained values are discussed below.

A value of 0.7 is used for ξ in this formalism, based on the mean temperature dependence of hydrogen and helium-broadened H_2O lines (Dutta *et al.* 1993). Note, however, that the temperature dependence of the linewidth on the opacity is relatively weak, so the value which is used is not especially critical. For instance, choosing the lower limit of 0.5 gives only an 8% change in attenuation at the lowest temperature (193 K) and in the farthest wings (S band), while the upper limit of 1 gives only a 14% change in opacity. We further assume that ξ is not a function of the broadening agent or of the spectral line.

The value of 1.96 GHz/bar for $\Delta\nu^0_{H_2}$ was taken from a measurement made by Joiner *et al.* (1992) near the 216 GHz rotational H_2S line at room temperature and is assumed to be the same for all lines. The helium broadening term ($\Delta\nu^0_{He}$) has been measured for the 168 GHz line (Willey *et al.* 1989) at room temperature and has a value of 1.20 GHz/bar and again is assumed constant for all rotational lines. The self-broadening term, $\Delta\nu^0_{H_2S}$, has been measured for four prominent millimeter lines by Helminger and DeLucia (1977), who report values of 5.38, 6.82, 5.82, and 5.08 GHz/bar for the 168, 216, 300, and 393 GHz rotational lines, respectively. For the rest of the lines the mean of these values (5.78 GHz/bar) will be used. With these values (of which the hydrogen broadening term is most crucial due to the prevalence of hydrogen in the atmosphere of the outer planets) the linewidth can be calculated for a given pressure, temperature, and composition.

For the remaining parameters, it was found that a best fit to these data has $\zeta = \gamma$, which is the upper limit for ζ since larger values force the lineshape function to be

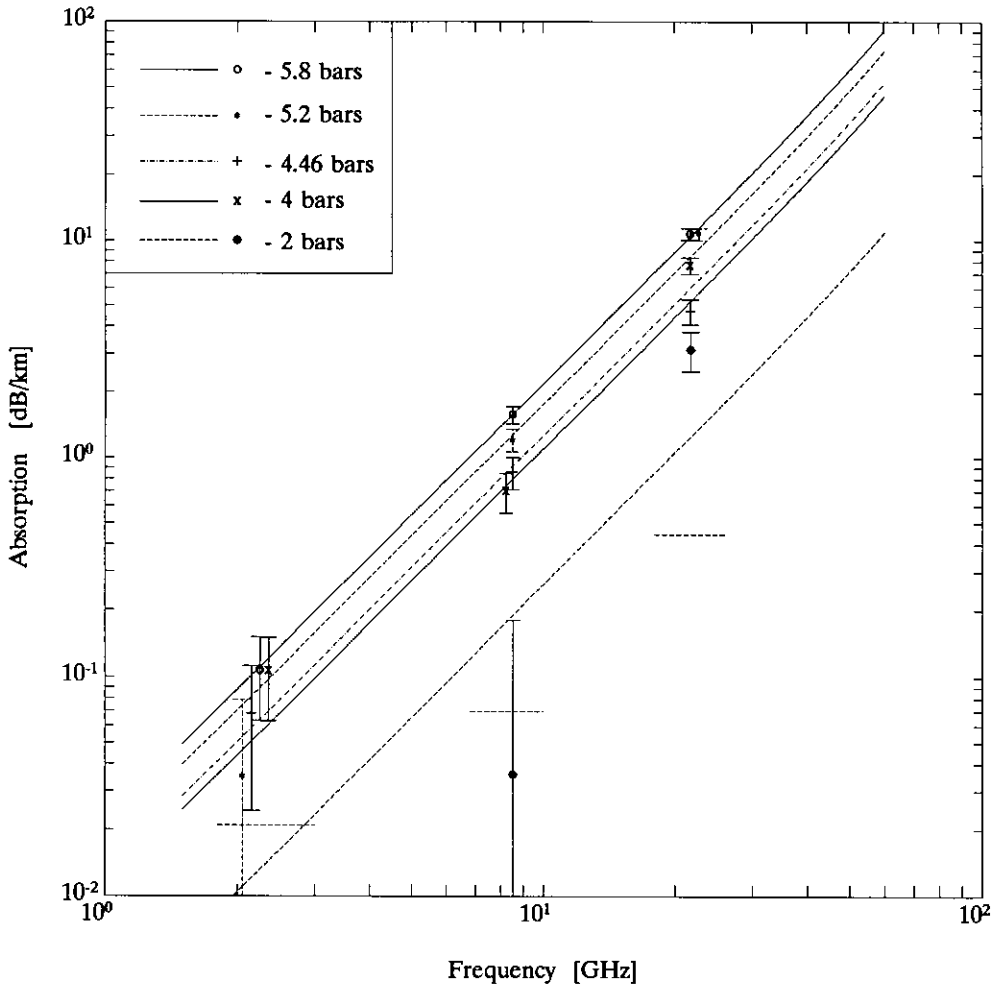

FIG. 4. H_2S attenuation under outer planet atmospheric conditions at 212 K. The theoretical curves are calculated from the Ben-Reuven lineshape function derived in this paper. The data points are data taken in March of 1994 and have been spread about the actual frequency for clarity. The horizontal dashed lines show the estimated average system sensitivity levels at the three bands.

negative under certain conditions. Furthermore, it is assumed that δ is a constant for all spectral lines, and is given by $\delta = \delta^0_{H_2S} P_{H_2S}$, which is analogous to the pressure shift form for ammonia (Berge and Gulkis 1976). A value of $\delta^0_{H_2S} = 1.28$ GHz/bar is derived from our laboratory measurements. Note that this formalism is almost a kinetic lineshape except for δ being nonzero (Gross 1955). Table IV gives a summary of the parameters for the formalism, while Figs. 2–5 show the results graphically.

For comparison, Fig. 6 shows this formalism as well as two Van Vleck–Weisskopf formalisms for the March 23, 1994 data at 212 K and 5.84 bars. The solid line is the Ben-Reuven formalism presented above, while the lowest (dashed) line is a Van Vleck–Weisskopf formalism assuming $\Delta\nu^0_{H_2} = 1.96$ GHz/bar. From Joiner *et al.* (1992), the largest value of $\Delta\nu^0_{H_2}$ consistent within their error bars is 2.43 GHz/bar and the Van Vleck–Weisskopf model using that value is the middle (dot–dashed) line. Both Van Vleck–Weisskopf models clearly understate the opacity in the wings, while the formalism presented in this work does a much better job. It is clear that despite some difficulties with the data this formalism is a significant improvement over prior models and will allow better analysis of radio astronomical data.

5. DISCUSSION

It is quite interesting that H_2S has relatively large values for both the real and imaginary parts of its dielectric constant. The normalized refractivity value of 8.85×10^{-17} N-units/molecule/cm^3 is nearly five times larger than that of CO_2 and the absorptivity is such that it possibly plays a role in determining the observed brightness temperature of the giant planets, particularly on Uranus and Neptune, where H_2S may be enhanced relative to ammonia (de Pater *et al.* 1991).

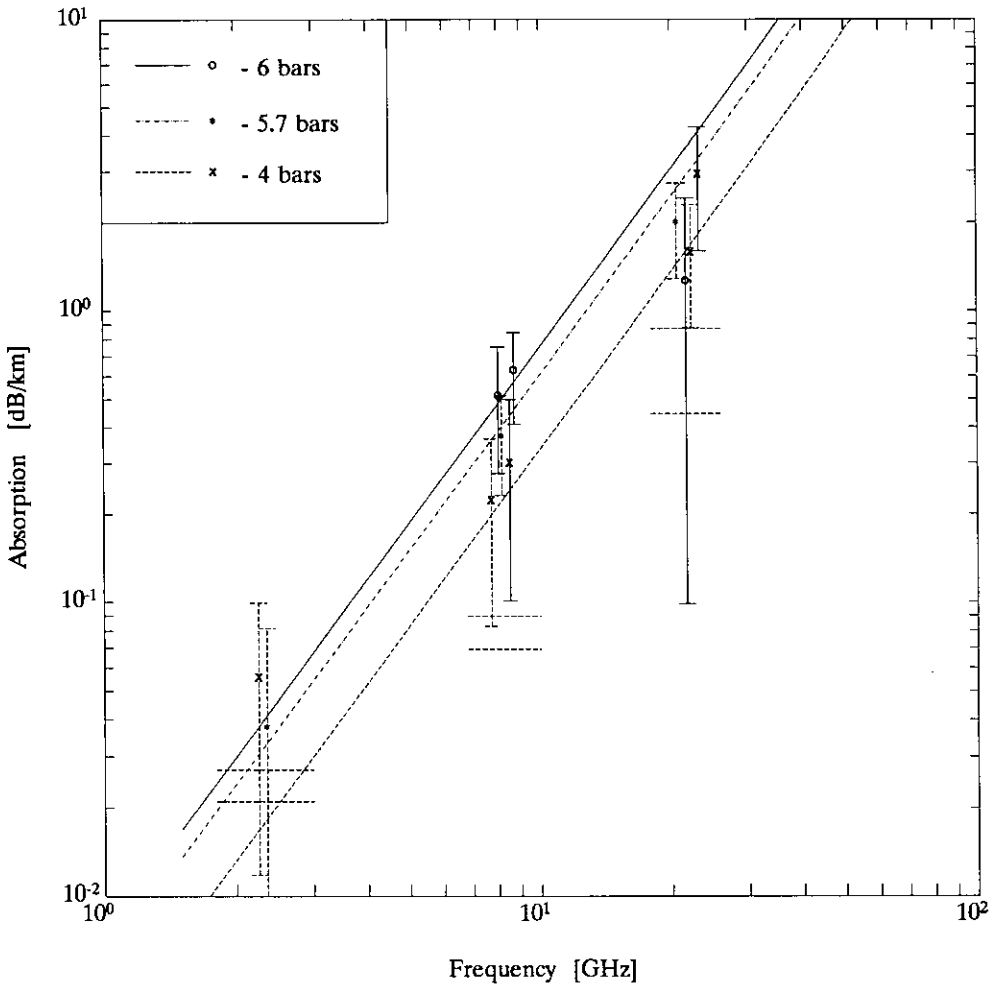

FIG. 5. H_2S attenuation under outer planet atmospheric conditions at room temperature. The theoretical curves are calculated from the Ben-Reuven lineshape function derived in this paper. The data points are representative of the full data set listed in Table III and have been spread about the actual frequency for clarity. The S band data taken prior to 1994 and the data at 2 bars have been left off for reasons explained in the caption of Fig. 2. The horizontal dashed lines show the estimated average system sensitivity levels at the three bands, the upper line being for the system prior to 1994 and the lower one for the system in March of 1994.

One immediate application of the proposed H_2S opacity formalism is to the radio occultation results of Neptune (Lindal 1992). Lindal postulated that the opacity measured at 6.3 bars and 135 K by Voyager 2 radio occultation of Neptune was due to NH_3 and from the radio occultation data derived a mixing ratio of 5×10^{-7}. Unfortunately the Voyager absorption profiles themselves seem to be lost, though efforts are being made to locate them, and the opacity must be determined from the stated ammonia mixing ratio. Using the Berge and Gulkis (1976) formalism for ammonia opacity as Lindal did, one derives the absorption at S band (2.3 GHz) to be 8.17×10^{-4} dB/km and at X band (8.4 GHz) to be 1.06×10^{-2} dB/km. The opacity then seemed to follow the ammonia saturation curve (Lindal 1992). The assumption that ammonia provides the absorption was made since it was believed that only ammonia had the intrinsic opacity to realistically explain the observed attenuation. However, it now appears possible that H_2S may itself be responsible for the opacity measured by Voyager 2.

If one postulates that H_2S is the agent producing the measured opacity at 6.3 bars, the absorption calculated from Lindal 1992 above yields an H_2S mixing ratio of 1.7×10^{-4}, using the formalism for H_2S opacity in this work. This mixing ratio yields S and X band absorption under Neptune conditions at 6.3 bars of 7.87×10^{-4} and 1.05×10^{-2} dB/km respectively. Furthermore, the measured absorption above 6.3 bars would also appear to follow the H_2S saturation vapor curve if responsible for the opacity, as evidenced by noting where H_2S in distributions (1)–(3) below (which assume that H_2S is responsible for the opacity) condenses out relative to ammonia in

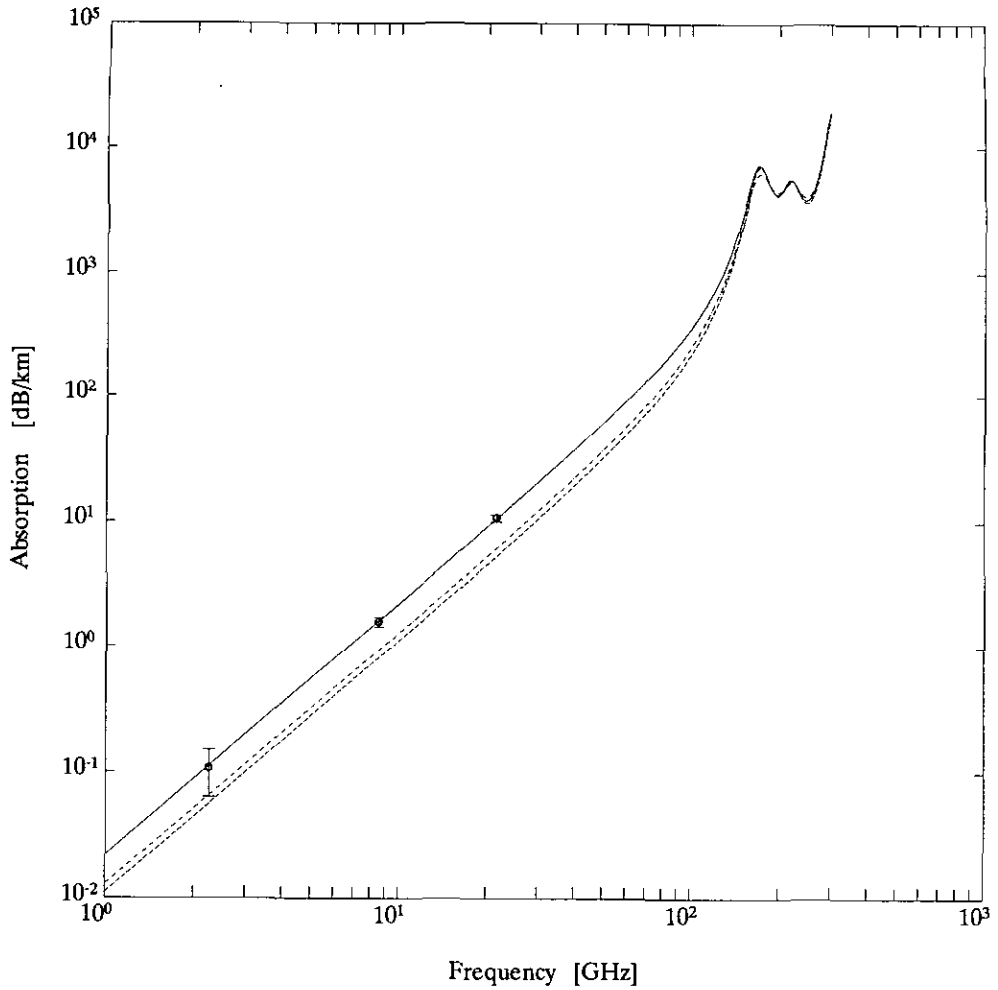

FIG. 6. The formalism in this paper (solid line) plotted against Van Vleck–Weisskopf formalisms with $\Delta\nu^0_{H_2}$ values of 1.96 (dashed line) and 2.43 (dot–dashed line) GHz/bar for 5.84 bars and 212 K. The Van Vleck–Weisskopf shape consistently understates the opacity by at least a factor of 2 off the line centers.

distribution (4) (which assumes that NH_3 is responsible—see Fig. 7). Note that there is nearly a constant differential between them above the deepest data from the Voyager radio occultation experiment, which allows both to explain the opacity. Again, it is unfortunate that the absorption profiles themselves are not currently accessible. If we assume that (1) NH_3 is present in solar abundance below the putative NH_4SH cloud, (2) the mixing ratio of H_2S is the mixing ratio of NH_3 plus 1.7×10^{-4}, and (3) H_2S completely depletes NH_3 in the NH_4SH cloud, then this requires the abundance of H_2S to be 8 times the solar sulfur value below the putative NH_4SH cloud (assuming the solar values of Anders and Grevesse 1989). This value of H_2S is similar to superabundances of H_2S previously postulated for Neptune (de Pater *et al.* 1991). Note that this is merely one test case to determine if the hypothesis of H_2S being the measured absorber in the upper troposphere is consistent with other observational data.

TABLE IV
H_2S Microwave Opacity Formalism

$$\gamma = \sum_i \gamma_i^0 P_i \left(\frac{T_0}{T}\right)^{\xi} \quad \zeta = \gamma \quad \delta = \delta^0_{H_2S} P_{H_2S}$$

ξ	0.7
$\gamma^0_{H_2}$	1.96
γ^0_{He}	1.20
$\gamma^0_{H_2S}$	5.78[a]
$\delta^0_{H_2S}$	1.28

[a] Used for all but the following lines: 168, 216, 300, and 393 GHz (see text).

The resulting spectrum of Neptune given the above distribution is shown in Fig. 8 (solid line) along with spectra calculated from similar distributions but with varying ammonia and hydrogen sulfide concentrations. The calcu-

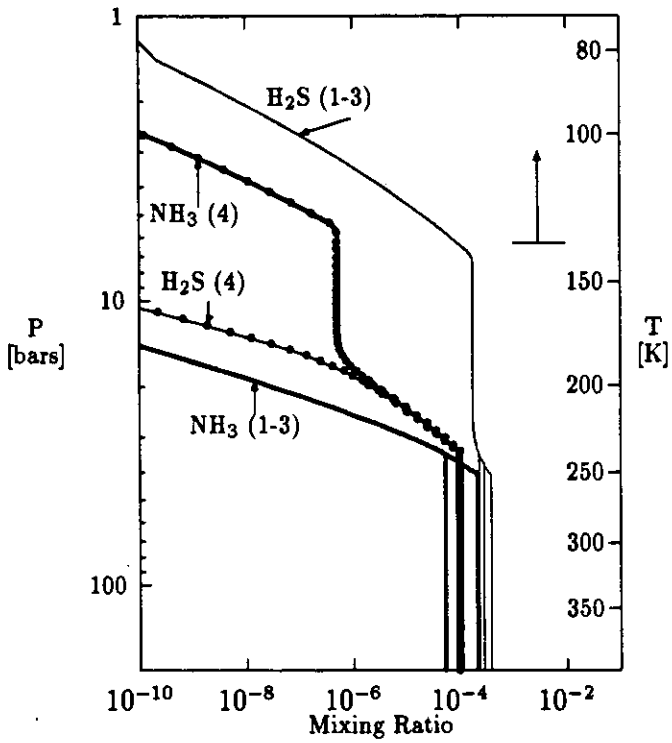

FIG. 7. Plot of H_2S and NH_3 distributions 1–4 from the text. Above the NH_4SH cloud (near 35 bars) distributions 1–3 are identical. The vertical arrow to the right shows the deepest penetration of the Voyager radio occultation experiment.

lated models assume the composition of Neptune's deep atmosphere to be 16 × solar H_2O, 30 × solar CH_4, and (1) one half solar NH_3 and 6 × solar H_2S (dot–dashed line); (2) solar NH_3 and 8 × solar H_2S (solid line); (3) 2 × solar NH_3 and 12 × solar H_2S (dashed line); and (4) solar NH_3 and 3 × solar H_2S (the dot–dashed line which does not merge near 5 GHz). The first three cases all keep the NH_3–H_2S difference a constant 1.7×10^{-4} above the NH_4SH cloud, while distribution (4) considers one case where the mixing ratio of ammonia is 5×10^{-7} above the NH_4SH cloud. Although the computed spectra using abundances (1)–(3) above and the new formalism for H_2S opacity are not entirely consistent with radio astronomical data (lying considerably above the much more reliable VLA data between 4 and 22 GHz), the possibility of H_2S playing an important role in the opacity of the upper troposphere of Neptune can not be ruled out. These abundance profiles will serve as a starting point for future investigations into the constituent abundances of Neptune.

Prior to these laboratory measurements it was believed that only ammonia had sufficient opacity to provide the attenuation observed by the Voyager 2 radio occultation experiments. We note now, however, that H_2S provides a possible explanation for the observed radio occultation absorption based on the laboratory data.

6. CONCLUSION AND SUGGESTIONS FOR FUTURE WORK

The laboratory analysis of H_2S under conditions simulating the outer planets show that this molecule contributes more opacity than was previously predicted using Van Vleck–Weisskopf line shapes, which tend to understate the opacity by a factor of two or more at centimeter wavelengths (see Fig. 6). Based on this, it is possible that H_2S may be an important microwave absorber in the upper troposphere ($\leq$ 6 bars) of Neptune.

The laboratory measurements taken represent the only centimeter wavelength measurements of H_2S under Jovian conditions and the formalism developed in this work provides a great improvement over previous models based on these laboratory measurements; however, certain problems are still evident. Chief among them are the lack of measurements under varying mixtures (additional measurements would allow a better estimate of the various gas components of the linewidth, line coupling, and pressure shift parameters) and the lack of complete frequency coverage. The suggested remedy is naturally more laboratory measurements.

Despite these shortcomings, the data and proposed new H_2S opacity formalism provide important and useful information in interpreting and processing a whole host of astronomical data: the application to Neptune radio occultation results is an example of this. More detailed analysis is being pursued in future work.

APPENDIX A. CALCULATING THE UNCERTAINTY OF OPACITY MEASUREMENTS

Define a quantity

$$\Psi = g(f_{0l}, \Delta f_l, f_{0u}, \Delta f_u) = \frac{\gamma_l \Delta f_l}{f_{0l}} - \frac{\gamma_u \Delta f_u}{f_{0u}}, \tag{24}$$

where Δf_l and Δf_u are the loaded and unloaded half power bandwidths and f_{0l} and f_{0u} are the loaded and unloaded center frequencies. We define this quantity since we wish to ignore the $1/\lambda$ dependence in front of the expression for α (Eq. (8)) in the interest of symmetry. Then to first order

$$\begin{aligned}\delta\Psi &= \frac{\partial g}{\partial f_{0l}}\delta f_{0l} + \frac{\partial g}{\partial \Delta f_l}\delta \Delta f_l + \frac{\partial g}{\partial f_{0u}}\delta f_{0u} + \frac{\partial g}{\partial \Delta f_u}\delta \Delta f_u \\ &= \frac{\gamma_u}{f_{0u}}\left[\frac{\Delta f_u \delta f_{0u}}{f_{0u}} - \delta \Delta f_u\right] - \frac{\gamma_l}{f_{0l}}\left[\frac{\Delta f_l \delta f_{0l}}{f_{0l}} - \delta \Delta f_l\right] \\ &= \Gamma_u - \Gamma_l.\end{aligned} \tag{25}$$

Note that this ignores variation in γ, which, from Eq. (8), is equal to $1 - \sqrt{t}$, as well as in the $1/\lambda$ term out front. The fractional change in γ can be expressed to first order as

$$\frac{\delta\gamma}{\gamma} = \frac{\delta t}{t}\left(\frac{1}{2 - 2/\sqrt{t}}\right). \tag{26}$$

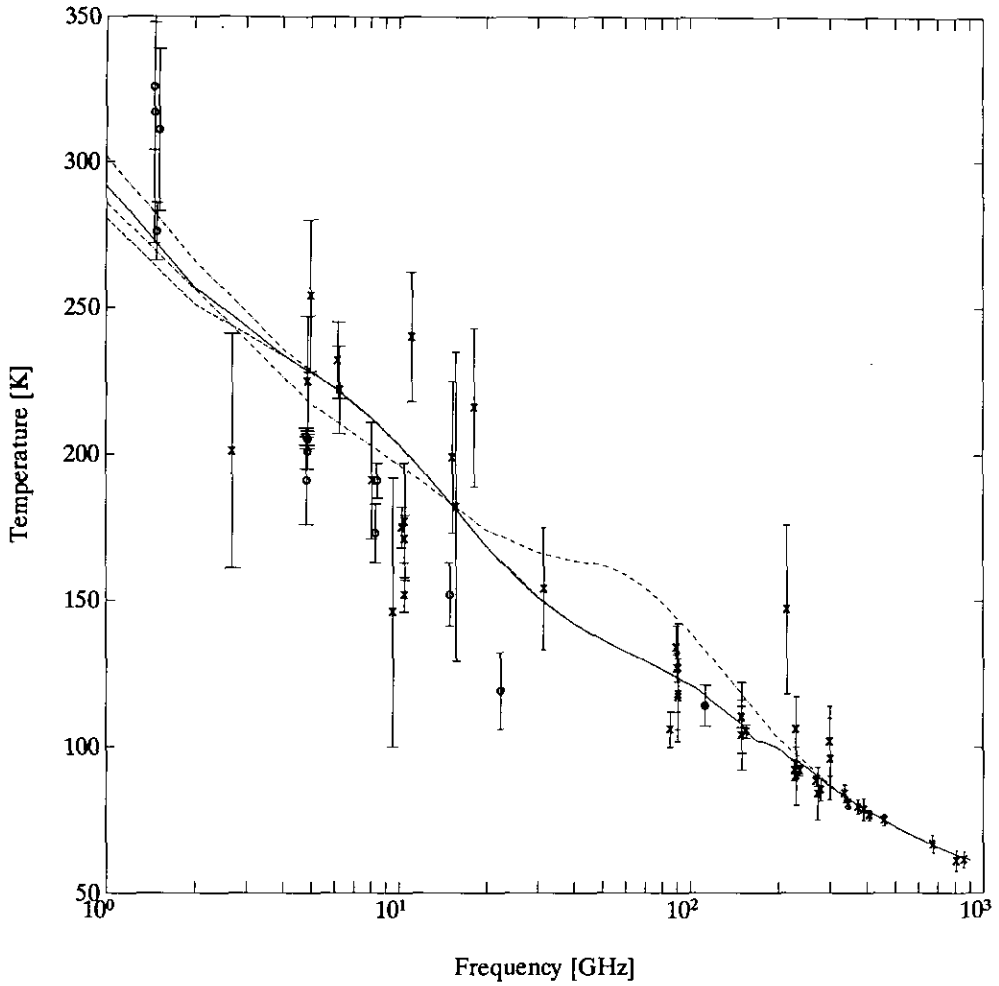

FIG. 8. Neptune's observed spectrum and model calculations with the deep constituent abundances given in the text. This model neglects the formation of an aqueous solution cloud and cloud opacity which may affect the spectrum at centimeter wavelengths (de Pater and Massie 1985). The 'x' data points are single dish data catalogued in de Pater and Richmond (1989) and Griffin and Orton (1993); the 'o' data points are VLA data from de Pater and Richmond (1989), de Pater *et al.* (1991), and Hofstadter (1993); and the filled circle is from Owens Valley (Muhleman and Berge 1991).

At K band, worst case values of $\delta t/t$ were on the order of 10% and therefore the fractional change of γ was less than 1%. Similarly for S band and X band measurements, worst case variations in γ were less than 1%. Also, as stated previously, the measurements of λ varied by less than 0.01% and therefore we see that to a good approximation we can neglect variation in those two terms.

Assume that $\langle \delta\Psi \rangle = 0$; that is, we are dealing with zero-mean processes. Therefore

$$\sigma_\Psi^2 = \langle \delta\Psi^2 \rangle = \langle \Gamma_u^2 \rangle + \langle \Gamma_l^2 \rangle - 2\langle \Gamma_l \Gamma_u \rangle, \tag{27}$$

where

$$\langle \Gamma_i^2 \rangle = \frac{\gamma_i^2}{f_{0i}^2}\left[\frac{\langle \delta f_{0i}^2 \rangle}{Q_i^2} + \langle \delta\Delta f_i^2 \rangle - \frac{2\langle \delta f_{0i}\delta\Delta f_i \rangle}{Q_i}\right] \quad i = u, l$$

$$\langle \Gamma_u \Gamma_l \rangle = \frac{\gamma_u \gamma_l}{f_{0l} f_{0u}}\left[\frac{\langle \delta f_{0l}\delta f_{0u} \rangle}{Q_l Q_u} + \langle \delta\Delta f_l \delta\Delta f_u \rangle - \frac{\langle \delta f_{0l}\delta\Delta f_u \rangle}{Q_l} - \frac{\langle \delta f_{0u}\delta\Delta f_l \rangle}{Q_u}\right]$$

$$Q_i = \frac{f_{0i}}{\Delta f_i} \quad i = u, l.$$

The bandwidth variation ($\delta\Delta f$) consists of instrument accuracy and noise; i.e., $\delta\Delta f_i = \delta\Delta f_{SA} + \delta\Delta f_{Ni}$, where $i = u, l$ for an unloaded and loaded resonator, respectively. Throughout, we will assume that electrical noise and the spectrum analyzer accuracy are uncorrelated. Since we have assumed zero-mean processes and uncorrelated accuracy and electrical noise contributions, then

$$\langle \delta f_{0i}^2 \rangle = \sigma_0^2 \tag{28}$$

$$\langle \delta\Delta f_i^2 \rangle = \sigma_\Delta^2 + \sigma_{Ni}^2, \tag{29}$$

where again i = u, l and the σ's are defined in Section 3. The 1σ uncertainty of the measured gas absorption, α, is then

$$\sigma = \pm\frac{8.686\pi}{\lambda}\sigma_\psi \quad \text{dB/m}, \tag{30}$$

where we have neglected the uncertainty in the measurement of λ and the transmissivity, t. There are three cases that we will consider: the uncorrelated case, the "worst" correlation case, and the "best" correlation case.

A.1. Uncorrelated Case

In the uncorrelated case, where naturally all variations are uncorrelated with one another, we find that

$$\langle\Gamma_i^2\rangle = \frac{\gamma_i^2}{f_{0i}^2}\left[\frac{\sigma_0^2}{Q_i^2} + \sigma_\Delta^2 + \sigma_{Ni}^2\right] \quad i = \text{u, l} \tag{31}$$

$$\langle\Gamma_l\Gamma_u\rangle = 0 \tag{32}$$

for the terms in Eq. (27).

A.2. Worst Case

In the worst case scenario (the greatest error), $\delta f_u\delta\Delta f_l$ and $\delta f_l\delta\Delta f_u$ terms are completely correlated while the other terms are completely anti-correlated and, of course, the electrical noise terms are uncorrelated with the instrument accuracy terms. This yields

$$\langle\Gamma_i^2\rangle = \frac{\gamma_i^2}{f_{0i}^2}\left[\frac{\sigma_0^2}{Q_i^2} + \sigma_\Delta^2 + \sigma_{Ni}^2 + \frac{2\sigma_0\sigma_\Delta}{Q_i}\right] \quad i = \text{u, l} \tag{33}$$

$$\langle\Gamma_u\Gamma_l\rangle = -\frac{\gamma_u\gamma_l}{f_{0l}f_{0u}}\left[\frac{\sigma_0^2}{Q_lQ_u} + \sigma_\Delta^2 + \frac{\sigma_0\sigma_\Delta}{Q_l} + \frac{\sigma_0\sigma_\Delta}{Q_u}\right]. \tag{34}$$

This is the case used for the quoted errors in this work, since those few small error terms (γ and λ) have been neglected in this derivation.

A.3. Best Case

The best case scenario is the inverse of the worst case; that is, $\delta f_u\delta\Delta f_l$ and $\delta f_l\delta\Delta f_u$ terms are completely anti-correlated, while the other terms are completely correlated. This yields

$$\langle\Gamma_i^2\rangle = \frac{\gamma_i^2}{f_{0i}^2}\left[\frac{\sigma_0^2}{Q_i^2} + \sigma_\Delta^2 + \sigma_{Ni}^2 - \frac{2\sigma_0\sigma_\Delta}{Q_i}\right] \quad i = \text{u, l} \tag{35}$$

$$\langle\Gamma_u\Gamma_l\rangle = \frac{\gamma_u\gamma_l}{f_{0l}f_{0u}}\left[\frac{\sigma_0^2}{Q_lQ_u} + \sigma_\Delta^2 + \frac{\sigma_0\sigma_\Delta}{Q_l} + \frac{\sigma_0\sigma_\Delta}{Q_u}\right] \tag{36}$$

and provides a lower bound on the uncertainty.

ACKNOWLEDGMENTS

The authors acknowledge the efforts of students George O. Hirvela, David Lashley, and Shady Suleiman in this effort, and thank Dr. Imke de Pater for suggestions that appear in this work, as well as the reviewers for their excellent suggestions. This work was supported by the Planetary Atmospheres Program of the National Aeronautics and Space Administration under Grant NAGW-533.

REFERENCES

ANDERS, E., AND N. GREVESSE 1989. Abundances of the elements: Meteoritic and solar. *Geochim. Cosmochim. Acta* **53,** 197–214.

BEN-REUVEN, A. 1966. Impact broadening of microwave spectra. *Phys. Rev.* **145,** 7–22.

BERGE, G. L., AND S. GULKIS 1976. Earth-based radio observations of Jupiter: Millimeter to meter wavelengths. In *Jupiter* (T. Gehrels, Ed.), pp. 621–692. Univ. of Arizona Press, Tucson.

DE PATER, I., AND S. T. MASSIE 1985. Models of the millimeter–centimeter spectra of the giant planets. *Icarus* **62,** 143–171.

DE PATER, I., AND M. RICHMOND 1989. Neptune's microwave spectrum from 1 mm to 20 cm. *Icarus* **80,** 1–13.

DE PATER, I., P. N. ROMANI, AND S. K. ATREYA 1991. Possible microwave absorption by H_2S gas in Uranus' and Neptune's atmospheres. *Icarus* **91,** 220–233.

DUTTA, J. M., C. R. JONES, T. M. GOYETTE AND F. C. DELUCIA 1993. The hydrogen and helium pressure broadening at planetary temperatures of the 183 and 380 GHz transitions of water vapor. *Icarus* **102,** 232–239.

GINZTON, E. L. 1957. *Microwave Measurements*. McGraw–Hill, New York.

GRIFFIN, M. J., AND G. S. ORTON 1993. The near-millimeter brightness temperature spectra of Uranus and Neptune. *Icarus* **105,** 537–547.

GROSS, E. P. 1955. Shape of collision-broadened spectral lines. *Phys. Rev.* **97,** 395–403.

HELMINGER, P., AND F. C. DELUCIA 1977. Pressure broadening of hydrogen sulfide. *J. Quant. Spectrosc. Radiat. Transfer* **17,** 751–754.

HEWLETT–PACKARD CORPORATION 1986. *Hewlett-Packard Manual for the HP 8562A/B.*

HOFSTADTER, M. D. 1993. Microwave imaging of Neptune's troposphere. *Bull. Am. Astron. Soc.* **25,** 1077.

JOINER, J., P. G. STEFFES, AND J. M. JENKINS 1989. Laboratory measurements of the 7.5–9.58 mm absorption of gaseous ammonia (NH_3) under simulated Jovian conditions. *Icarus* **81,** 386–395.

JOINER, J., P. G. STEFFES, AND K. S. NOLL 1992. Search for sulfur (H_2S) on Jupiter at millimeter wavelengths. *IEEE Trans. Microwave Theory Tech.* **40,** 1101–1109.

LINDAL, G. F. 1992. The atmosphere of Neptune: An analysis of radio occultation data acquired with Voyager 2. *Astron. J.* **103,** 967–982.

MATTHAEI, G. L., L. YOUNG, AND E. JONES 1980. *Microwave Filters, Impedance-Matching Networks and Coupling Structures.* McGraw–Hill, New York.

MUHLEMAN, D. O., AND G. L. BERGE 1991. Observations of Mars, Uranus, Neptune, Io, Europa, Ganymede, and Callisto at a wavelength of 2.66 mm. *Icarus* **92,** 263–272.

PAPOULIS, A. 1991. *Probability, Random Variables, and Stochastic Processes,* 3rd ed. McGraw–Hill, New York.

POYNTER, R. L., AND H. M. PICKETT 1985. Submillimeter, millimeter, and microwave spectral line catalog. *Appl. Opt.* **24,** 2235–2240.

POZAR, D. M. 1990. *Microwave Engineering,* Addison–Wesley, Reading, MA.

PRESS, W. H., S. A. TEUKOLSKY, W. T. VETTERLING, AND B. P. FLANNERY 1992. *Numerical Recipes in C, The Art of Scientific Computing,* 2nd ed. Cambridge Univ. Press, London/New York.

REITZ, J. R., F. J. MILFORD, AND R. W. CHRISTY 1980. *Foundations of Electromagnetic Theory.* Addison–Wesley, Reading, MA.

SPILKER, T. R. 1990. *Laboratory Measurements of Microwave Absorptivity and Refractivity Spectra of Gas Mixtures Applicable to Giant Planet Atmospheres.* Ph.D. dissertation, Stanford.

SPILKER, T. R. 1993. New laboratory measurements on ammonia's inversion spectrum, with implications for planetary atmospheres. *J. Geophys. Res.* **98,** 5539–5548.

STEFFES, P. G., AND J. M. JENKINS 1987. Laboratory measurements of the microwave opacity of gaseous ammonia (NH_3) under simulated conditions for the jovian planets. *Icarus* **72,** 35–47.

TOWNES, C. H., AND A. L. SCHAWLOW 1955. *Microwave Spectroscopy.* Dover, New York.

TYLER, G. L., AND H. T. HOWARD 1969. Refractivity of carbon dioxide under simulated Martian conditions. *Radio Sci.* **4,** 899–904.

WILLEY, D. R., T. M. GOYETTE, W. L. EBENSTEIN, D. N. BITTNER, AND F. C. DELUCIA 1989. Collisionally cooled spectroscopy: Pressure broadening below 5 K. *J. Chem. Phys.* **91,** 122–125.